Cement & Concrete Composites 33 (2011) 513–519

Contents lists available at ScienceDirect

Cement & Concrete Composites

journal homepage: www.elsevier.com/locate/cemconcomp

Bond strength of corroded steel bars in reinforced concrete structural elements strengthened with CFRP sheets

Xiao-gang Wang [a,*], Wei-ping Zhang [b], Wei Cui [b], Folker H. Wittmann [c]

[a] Yantai University, School of Civil Engineering, China
[b] Tongji University, Department of Structural Engineering, China
[c] Qingdao Technological University, China

ARTICLE INFO

Article history:
Received 16 February 2010
Received in revised form 9 February 2011
Accepted 10 February 2011
Available online 15 February 2011

Keywords:
Bond
Steel reinforcement
Concrete
Corrosion
CFRP strengthening

ABSTRACT

The effectiveness of CFRP strengthening to maintain and enhance bond between corroded steel reinforcement and concrete has been investigated through pullout tests. Results indicate that strengthening with CFRP can increase the ultimate bond strength of specimens containing corroded steel reinforcement especially at medium or high levels of corrosion. The failure mode changes under these conditions from brittle bond splitting to more ductile rebar pullout in most cases. The confining effect of CFRP increases with increasing ratio of cover depth to rebar diameter c/d_b up to a value of about 2.3. But the confining effect is reduced if c/d_b increases beyond this value. Ultimate bond strength in specimens, which are strengthened before corrosion starts, can be significantly increased up to a degree of corrosion of about 15%. This beneficial effect cannot be observed if structural elements are strengthened after considerable corrosion took place already because in this case corrosion products can leak out of the interfacial zone into expansion cracks. Under these conditions, the reactionary confinement is reduced.

1. Introduction

Bond deterioration between steel reinforcement and concrete is one of the main reasons for structural degradation of corroded RC beams [1,2]. Both flexural capacity and ductile behavior are impaired by corrosion induced bond weakening. If insufficient anchorage is provided, as in the case of beams with curtailed bars, bond deterioration may result in serious anchorage failure and become the primary cause for reduction of flexural strength [3]. In order to fulfill the requirement for flexural performance evaluation of corroded RC beams, a number of studies have been undertaken in order to evaluate the effect of corrosion of reinforcement on bond between steel and concrete [4–7]. These studies have shown that bond strength first increases with ongoing corrosion up to a certain level before expansive cover cracking takes place. Further increase of corrosion, however, leads to progressive reduction of bond strength.

During the last decade, use of FRP material to repair or strengthen corrosion-damaged beams was strongly advocated [8–10]. However, little information can be found in the literature on the confining effect of FRP on bond between corroding/corroded steel bars and concrete so far. A pilot study has shown that the bond strength and slip-initiation load can be increased significantly by FRP strengthening, and that failure mode tends to change from bond splitting to bar pullout [11]. A modest number of specimens were tested only and no quantitative results were obtained.

FRP strengthening could potentially be an efficient way to prevent corrosion-related bond slippage and increase the bond strength. The objective of this study, therefore, is to further investigate the confining effect of FRP strengthening experimentally, and to develop a model based on results taken from literature and from the experimental series described in this manuscript.

2. Experimental

2.1. Test specimens

Twenty-nine pullout specimens are prepared for this test program, and variables mainly include corrosion degree and clear cover thickness, as shown in Table 1. The specimens can be subdivided into four groups:

(1) Group U consisted of six specimens, one control (uncorroded and unstrengthened), five were corroded to different levels and remained unstrengthened. (2) Group S consisted of fourteen specimens with different cover thickness, three uncorroded and strengthened, eleven corroded to different levels and strengthened. (3) Group P consisted of six specimens which were first strengthened with CFRP and then corroded. (4) Group R consisted of three specimens, they were corroded to a mass loss of 5% before strengthening, and exposed to further corrosion.

* Corresponding author. Tel.: +86 535 6902606.
E-mail address: wxgnet@163.com (X.-G. Wang).

0958-9465/$ - see front matter © 2011 Elsevier Ltd. All rights reserved.
doi:10.1016/j.cemconcomp.2011.02.008

Notation

c/d_b	ratio of cover depth to rebar diameter	τ_{uc0}	deteriorated bond strength between corroded steel bar and concrete
t	time	τ_u	bond strength between concrete and steel bar without corrosion
Z	valency of reaction anode	k_u	coefficient related to c/d_b
F	Faraday's constant	τ_{uc}	deteriorated bond strength between corroded rebar and confined concrete
A	atomic mass of iron	τ_{uc1}	bond strength from contribution of stirrup and CFRP confinement
I	current density		
ρ	density of iron		
R	radius of reinforcing bar		
η_s	mass loss ratio of steel bar		

Table 1
Characterization of test specimens.

Group	Cover thickness (mm)	Mass loss					
		0	3%	5%	7%	10%	15%
U	25	25-U0	25-U3	25-U5	25-U7	25-U10	25-U15
S	15	15-S0	15-S3		15-S7		15-S15
	25	25-S0	25-S3	25-S5	25-S7	25-S10	25-S15
	35	35-S0	35-S3		35-S7		35-S15
P	25	25-P0	25-P3	25-P5	25-P7	25-P10	25-P15
R	25				25-R7	25-R10	25-R15

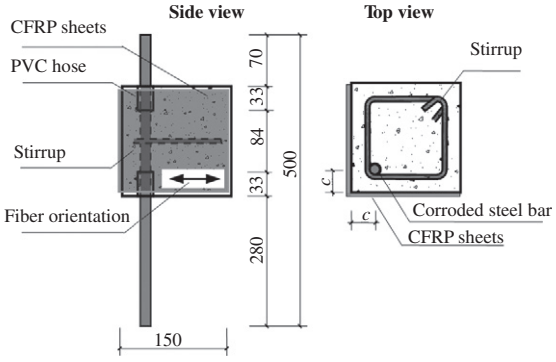

Fig. 1. Schematic view of pullout specimens.

Fig. 1 shows a schematic view of the pullout specimens. Deformed steel bars with a diameter of 14 mm were placed in one corner of concrete cubes with the following dimension: 150 mm × 150 mm × 150 mm. The center part of the reinforcing bars with a length of 84 mm was bonded to concrete. The steel bar was not bonded to the concrete at the top and the bottom over a length of 33 mm respectively, however. There the steel bar was covered by a PVC hose. In this way movement of the reinforcing bar was not influenced by the confining pressure of concrete due to the action of the support. Round bar with a diameter of 6 mm was selected for closed stirrups, which were placed right at half height of the specimens but isolated from the main bar to avoid corrosion. This was set particularly to avoid damage of seriously corroded specimens during strengthening process.

2.2. Material properties

The constituents of the concrete used for the preparation of the pullout specimens consisted of ordinary Portland cement, sand with a maximum diameter of 5 mm, coarse aggregate with a maximum diameter of 15 mm and tap water. The water, cement, sand, coarse aggregate ratio was fixed to be 1:2:2.98:6.33. The 28 days axial compressive strength of concrete was found to be 24.0 MPa on an average. Yield strength, ultimate strength and elastic modulus of the steel bars are 374 MPa, 571 MPa and 210 GPa respectively. The thickness of the CFRP sheets used in these tests is 0.167 mm. Tensile strength, elastic modulus and ultimate elongation of the used CFRP laminates are 4193 MPa, 261.8 GPa and 1.7% respectively.

2.3. Accelerated corrosion test setup

Pullout specimens were cured in room temperature for 28 days. Then they were placed into glass tanks, as shown in Fig. 2, immersed in a 5% NaCl solution. The solution level in the tanks was controlled to be about 40 mm lower than the lower surface of the steel reinforcement. A copper slice was used as cathode and the corroding reinforcement bars served as anode. A constant current was applied during the corrosion process to generate a constant current density of 200 μA/cm^2.

Based on Faraday's law, the required duration of the accelerated corrosion process can be expressed as a function of applied current density and predefined corrosion degree as follows,

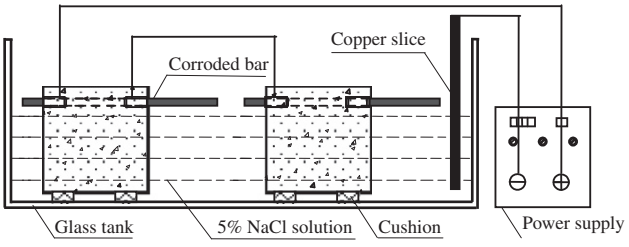

Fig. 2. Schematic view of the accelerated corrosion test set-up.

$$t = \frac{ZF \cdot r \cdot \rho\eta_s}{2A \cdot i} \quad (1)$$

where t is time of corrosion (s), Z is the valency of the reacting anode, which is 2 in this case (iron), F is Faraday's constant (F = 96,500 A s), r is the radius of corroded bar (cm), ρ is the density of iron (ρ = 7.87 g/cm^3), η_s is the mass loss ratio, A is the atomic mass of iron (A = 56 g), and i is the current density (A/cm^2).

2.4. Strengthening method

A single ply of CFRP sheet measuring 140 mm by 300 mm was used for strengthening, as shown in Fig. 1. It was bonded to the two surfaces closest to the steel bar instead of circumferential wrapping in order to simulate practical situation. Fibers were oriented in the direction perpendicular to the main bar.

The process of applying CFRP to concrete includes four steps: (1) surface preparation, (2) resin under-coating, (3) CFRP applying, and (4) resin over-coating. The two surfaces were prepared by sand blasting followed by cleaning. The corner over which CFRP was applied was ground to a radius of 6 mm. After this first step epoxy resin was applied to the prepared concrete surfaces. CFRP sheets were pressed on the surfaces after the epoxy resin began to be dry. Finally, a resin over-coating was applied over the CFRP sheets. Complete curing took one week at room temperature.

2.5. Pullout test setup

A loading frame was designed and fabricated to perform the pullout tests, as shown in Fig. 3. The upper rod was fixed to the base of an Instron universal testing machine and supported the weight of specimens and of the loading frame by a hemispherical bearing. Pullout specimens were placed on the reaction plate with the main reinforcement bar passing through the central hole.

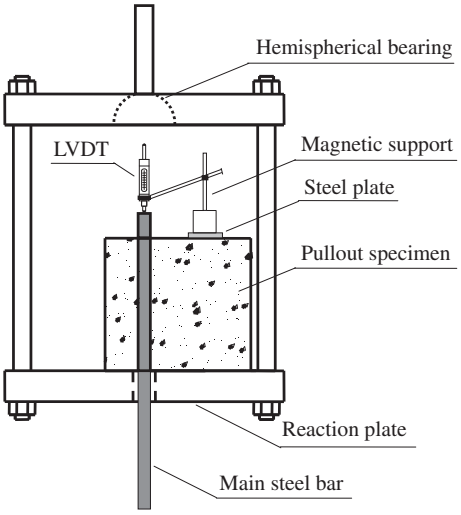

Fig. 3. Loading test frame.

A linear variable differential transformer (LVDT) was applied to monitor the free-end slip. The data from the LVDT together with the pullout load were collected by a computer. Load was applied manually at a rate of 0.2 kN per second, up to failure.

3. Test results and discussion

3.1. Bond strength and failure modes

Bond strength is the maximum average bond stress, which is calculated through dividing applied force by the bonded rebar surface area. All test results are compiled in Table 2. Since the

Table 2
Compilation of test results.

Type of specimen	Mass loss	Ultimate bond stress (MPa)	Slip initiation bond stress (MPa)	Slip at ultimate load (mm)	Failure mode
25-U0	–	7.13	4.18	1.227	Pullout
25-U3	0.025	7.21	5.98	0.221	Splitting
25-U5	0.043	6.80	6.06	1.643	Pullout
25-U7	0.068	5.22	5.05	0.744	Splitting
25-U10	0.093	5.70	5.70	0.103	Splitting
25-U15	0.137	4.52	3.54	0.806	Splitting
15-S0	–	5.90	5.49	0.485	Pullout
15-S3	0.021	5.24	4.42	1.196	Pullout
15-S7	0.069	5.82	4.82	2.428	Pullout
15-S15	0.262	4.42	4.42	0.076	Splitting
25-S0	–	6.23	4.96	1.698	Pullout
25-S3	0.017	6.39	6.39	0.038	Pullout
25-S5	0.035	6.96	6.96	0.118	Pullout
25-S7	0.065	12.39	12.39	0.091	Pullout
25-S10	0.134	9.24	9.24	0.246	Pullout
25-S15	0.178	10.42	10.42	0.222	Pullout
35-S0	–	9.91	8.19	1.269	Pullout
35-S3	0.005	5.74	4.84	1.329	Pullout
35-S7	0.047	11.56	11.56	0.095	Pullout
35-S15	0.128	9.24	9.24	0.109	Splitting
25-P0	–	6.23	4.17	1.698	Pullout
25-P3	0.019	6.97	5.57	1.095	Pullout
25-P5	0.034	11.90	11.90	0.118	Pullout
25-P7	0.063	13.83	13.83	0.011	Pullout
25-P10	0.084	11.89	11.89	0.084	Pullout
25-P15	0.168	16.51	16.51	0.21	Splittin[a]
25-R7	0.053	10.36	8.62	0.153	Pullout
25-R10	0.150	–	–	–	Bar rupture
25-R15	0.179	8.35	6.78	0.313	Splitting[a]

[a] CFRP peeled off after splitting cracking.

(a) splitting (25-U7) (b) pull-out (25-S15)

Fig. 4. Examples for the different failure modes.

Fig. 5. CFRP sheets Peeling off during splitting failure of specimen 25-R15.

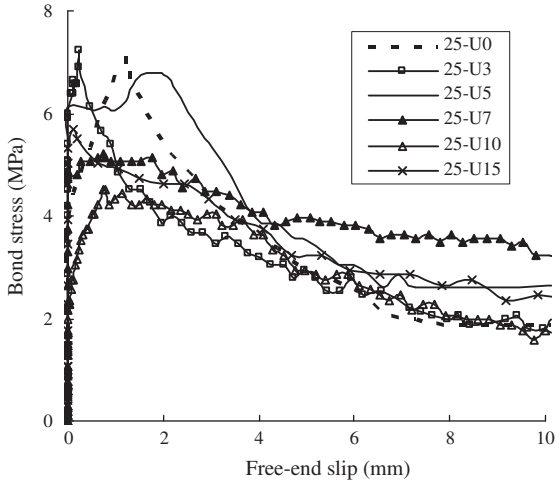

Fig. 6. Bond stress versus free-end slip relations as observed on unstrengthened specimens.

corrosion degree cannot be predicted very precisely by means of Faraday's law, the center part of the corroded steel bars was freed of concrete after the pullout test and the actual mass loss was measured. Values obtained in this way are listed in Table 2.

Three main failure modes could be observed during the pullout testing: (1) rebar pullout, (2) bond splitting and (3) rebar rupture. Typical examples of the failure modes are shown in Fig. 4. The combination of cover thickness, corrosion level and CFRP strengthening controlled the type of failure. Most unstrengthened specimens failed by bond splitting, which typically consisted of a brittle crack formed at the same location where a corrosion induced expansion crack existed already, as shown in Fig. 4a. Transverse confinement provided by CFRP strengthening can effectively prevent bond splitting cracks, and the majority of strengthened specimens failed by rebar pullout. However, the effect of CFRP is significantly weakened after severe corrosion took place. It is clear from Table 2 that nearly all the specimens with highest corrosion level failed by bond splitting despite high cover thickness and CFRP strengthening. In addition, opening of a splitting crack in strengthened specimens creates a complex state of stress with high tensile and shear stresses in the interface between CFRP sheets and concrete. This situation can lead to peeling off of CFRP sheets, as shown in Fig. 5.

Based on the test results presented in Table 2, it can be concluded that CFRP strengthening generally increased the ultimate bond stress significantly and changed the failure mode from brittle bond splitting to more ductile rebar pullout.

3.2. Bond deterioration of unstrengthened specimens

Fig. 6 shows load versus free-end slip relationships for unstrengthened specimens having different degrees of corrosion. It can be seen that maximum bond stress hardly decreases up to a degree of corrosion of 5%. Bond strength of specimen 25-U3 even had a slightly increased bond strength as compared with specimen 25-U0 without corrosion. This phenomenon has been observed by several authors before and can be well explained [6,12]. Once the degree of corrosion of a steel bar in concrete exceeds this limit bond strength drops gradually with continuing corrosion. At the same time the failure mode changed from rebar pullout to bond splitting.

Although corrosion induced bond deterioration has been studied intensively by many authors, it is still hard to establish a generally acceptable deterioration model. This is at least partly due to major differences in the applied testing methods. We know by now that differences in the accelerated corrosion techniques, in relative rib area loss of different diameter bars, in geometrical configuration of the specimens, and properties of the materials involved will have an immense influence on bond deterioration. Specific bond strength can be defined as the ratio of deteriorated bond strength and the bond strength observed in reference specimens without corrosion. The relation between specific bond strength and degree of corrosion obtained from published data are summarized in Fig. 7, comparable test configurations can be found in Table 3. It can be seen immediately that results obtained by different authors show large scatter. This is most probably essentially due to the differences in carrying out the experiments as mentioned above. Predictions according to Yuan's model [13] are also shown in Fig. 7. The straight line shown in Fig. 7 can be expressed by the following equations:

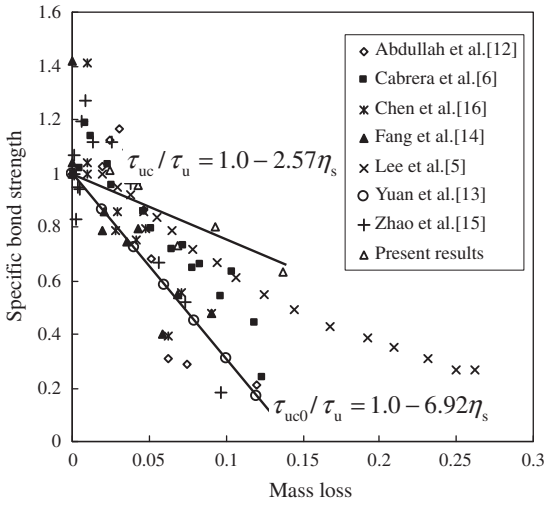

Fig. 7. Specific bond strength as function of mass loss due to corrosion as measured on unstrengthened specimens.

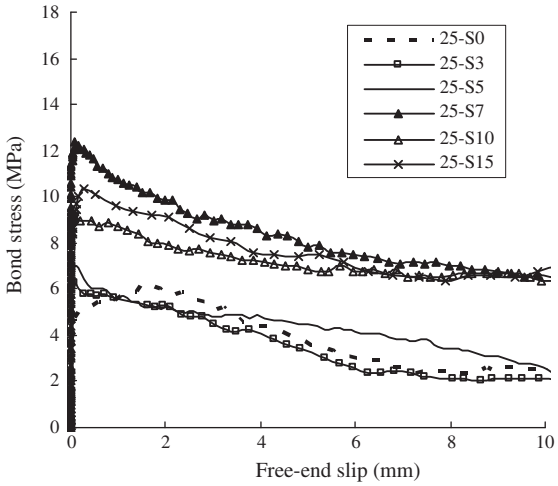

Fig. 8. Bond stress versus free-end slip relations for corroded and strengthened specimens with 25 mm cover.

$$\tau_{uc0}/\tau_u = (1.0 - k_u \cdot \eta_s) \quad (2)$$

$$k_u = 10.544 - 1.586 \times (c/d_b) \quad (3)$$

where τ_{uc0} stands for the deteriorated bond strength between corroded steel bar and concrete, τ_u for the bond strength between concrete and steel bar without corrosion, c for the cover thickness, d_b for the rebar diameter. k_u is a coefficient related to c/d_b, which can be calculated by Eq. (3). By means of Yuan's model a rather conservative prediction is obtained. It should be noted that Yuan's results as shown in Fig. 7 correspond to a specific value of $c/d_b = 2.3$. This value is valid for the series 25-U.

Our results as shown in Fig. 7 can also be approximated by a linear function. By means of a regression analysis we obtain Eq. (4).

$$\tau_{uc}/\tau_u = 1.0 - 2.57\eta_s \quad (4)$$

where τ_{uc} stands for the deteriorated bond strength between corroded rebar and confined concrete. Compared with Yuan's model described above, the corrosion induced bond deterioration as observed with our experimental set-up is less severe. The confinement with a stirrup may be one reason for this discrepancy.

3.3. Confining effects of CFRP strengthening

Fig. 8 shows the bond stress versus free-end slip relations for corroded and then strengthened specimens with a cover thickness of 25 mm. Compared with the results of unstrengthened corroded specimens (Table 2 and Fig. 6), it can be seen that ultimate bond strength is hardly improved by CFRP strengthening at a relative low degree of corrosion. However, substantial increase of ultimate bond strength is observed on strengthened specimens under medium and high levels of corrosion. At a degree of corrosion of 6.5% and 13.5% the improvement can be as high as 137% and 104% respectively.

Fig. 9 represents the specific bond stress as observed on strengthened specimens as a function of the mass loss ratio. Besides the increase of absolute bond strength mentioned above, the specific bond strength of 25-S series increased nearly linearly with increasing degree of corrosion. The result of a regression

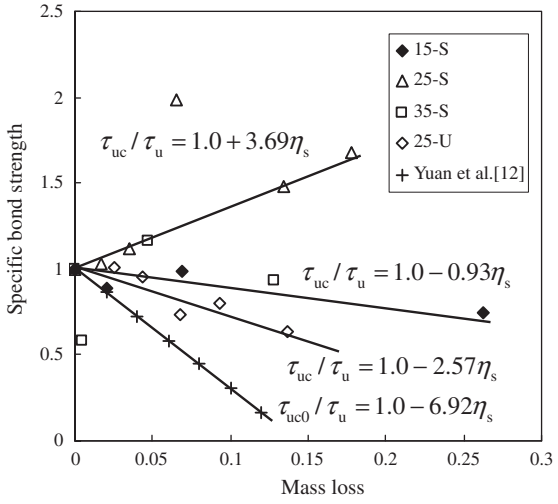

Fig. 9. Specific bond strength for unstrengthened and strengthened specimens as function of mass loss.

Table 3
Test configurations of comparable studies in the literature.

References	Testing methods	Impressed current density	Concrete compressive strength (MPa)	Rebar diameter (mm)	c/d_b	Bonded length
Abdullah et al. [12]	Cantilever test	10.4 mA/cm^2	30	12	5	$8d_b$
Cabrera and Ghoddoussi [6]	Pullout test	Unknown	–	12	5.5	$4d_b$
Chen et al. [16]	Pullout test	Unknown	39.1	20	3	$4d_b$
Fang et al. [14]	Pullout test	Unknown	37.6	20	3	$4d_b$
Lee et al. [5]	Pullout test	Unknown	24.7–42.1	13	2.5	$6d_b$
Yuan et al. [13]	Pullout test	1–2 mA/cm^2	24.7	14/18/20	2.3/1.9/1.8	$2.5d_b$
Zhao and Jin [15]	Pullout test	Unknown	16.8	12	3.6	$7d_b$
Present results	Pullout test	0.2 mA/cm^2	24.0	14	1.6/2.3/3.0	$6d_b$

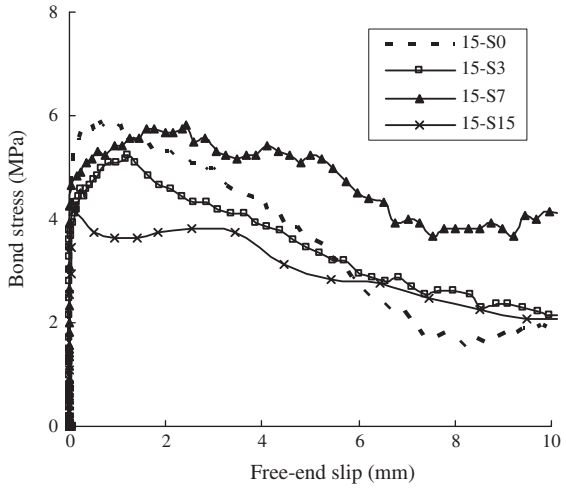

Fig. 10. Bond stress versus free-end slip curves for corroded and strengthened specimens with 15 mm cover.

analysis of the measured data is as shown in the following equation:

$$\tau_{uc}/\tau_u = 1.0 + 3.69\eta_s \quad (5)$$

This phenomenon is astonishing but it may be explained by the coupling effect of stirrup and CFRP confinement. The expansion pressure of the corrosion products on the surrounding concrete cannot be released completely by cracking of the cover due to confinement by the stirrup. Thus higher residual unreleased pressure can be accumulated under high level of corrosion. Since failure by bond splitting can be prevented effectively by CFRP strengthening, the stronger confinement and mechanical interlocking eventually lead to higher ultimate bond strength.

Bond stress versus free-end slip curves for specimens with 15 mm and 35 mm cover are presented in Figs. 10 and 11. It can be seen that the ratio of cover thickness to rebar diameter (c/d_b) has a distinct effect on ultimate bond strength. Strengthened specimens with a cover thickness of 15 mm and corroded to various levels all failed at bond stress below 6 MPa. Specimens with a cover thickness of 25 mm failed at a bond stress ranging from 6.23 MPa to 12.39 MPa, and the specimens with a cover thickness of 35 mm failed at a bond stress around 10 MPa except specimen 35-S3, which failed at a unreasonable low value of 5.74 MPa, most probably due to an undetected defect.

The confinement effect of CFRP strengthening under different corrosion levels is also considerably affected by the ratio c/d_b. As shown in Fig. 9, specific bond strength of specimens with a cover thickness of 15 mm does not increase with progressing corrosion but slightly decreases instead. By linear regression the following equation has been obtained:

$$\tau_{uc}/\tau_u = 1.0 - 0.93\eta_s \quad (6)$$

Large cover depth can reduce rate of bond deterioration, which is expressed by means of Eqs. (1) and (2), on the other hand the confining effect of CFRP is reduced [11]. Generally on specimens with a cover thickness of 35 mm the effect of corrosion was not really obvious in this research project. Thus Eq. (7) can be obtained,

$$\tau_{uc}/\tau_u = 1.0 \quad (7)$$

In order to fully understand the influence of the ratio c/d_b, the ultimate bond strength between concrete and corroded rebar was simplified into two parts: (a) bond strength provided by plain concrete τ_{uc0} and (b) contribution of stirrup and CFRP confinement τ_{uc1}. Specific bond strength τ_{uc}/τ_u is given as a function of mass loss ratio by Eq. (5), Eqs. (6) and (7) for specific c/d_b ratios. The following values have been found: 1.6 for the 15-S series, 2.3 for the 25-S series, and 3.0 for the 35-S series. Specific bond strength τ_{uc0}/τ_u at corresponding c/d_b ratio can be also expressed as function of mass loss ratio by Yuan's model [13] mentioned above. Thus specific bond strength τ_{uc1}/τ_u can be achieved by subtracting τ_{uc0}/τ_u from τ_{uc}/τ_u. The corresponding values are given in the following equations.

$$\tau_{uc1}/\tau_u = 7.12\eta_s \quad c/d_b = 1.6 \quad (8)$$

$$\tau_{uc1}/\tau_u = 10.62\eta_s \quad c/d_b = 2.3 \quad (9)$$

$$\tau_{uc1}/\tau_u = 5.79\eta_s \quad c/d_b = 3.0 \quad (10)$$

As these results have been obtained from a limited number of specimens application is largely limited, but it can be seen from the obtained values that an increase of the ratio c/d_b can improve the confining provided by stirrup and CFRP strengthening effect within a certain range. This observed effect will be reduced, however, with further increase of the ratio c/d_b beyond the limited

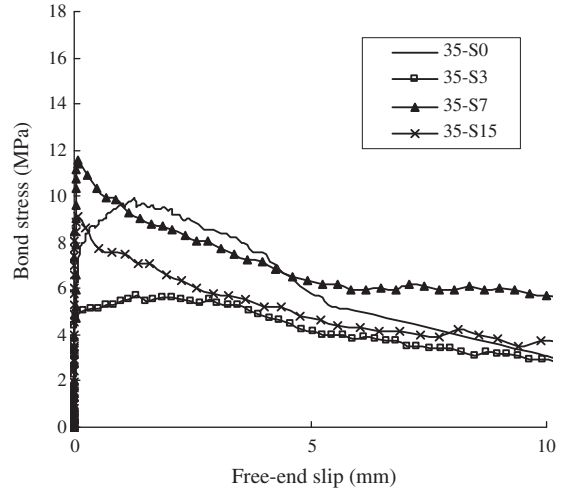

Fig. 11. Bond stress versus free-end slip curves for corroded and strengthened specimens with 35 mm cover.

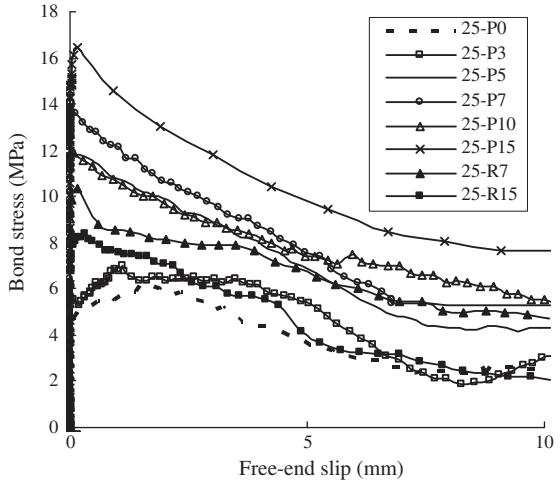

Fig. 12. Bond stress versus free-end slip curves for 25-P and 25-R series.

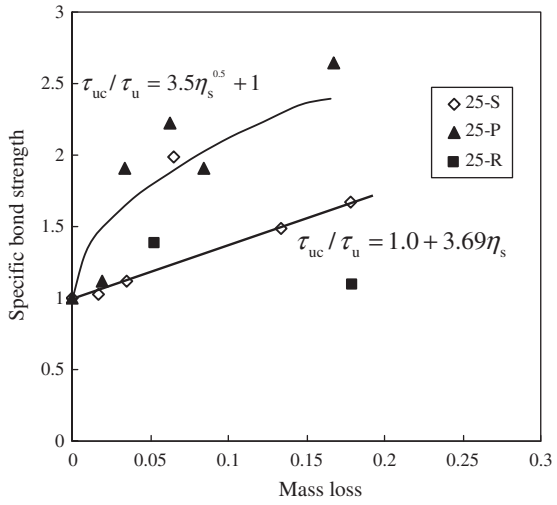

Fig. 13. Specific bond strength for 25-P and 25-R series.

range. Due to the limitation of the present work, precise threshold values of the ratio c/d_b cannot be fixed at this moment. However, the achieved results allow us an approximate estimation.

3.4. Bond degradation of strengthened specimens

The 25-P series was designed to investigate the bond deterioration under CFRP confinement. This should give us some ideas on long-term performance of structural members strengthened with CFRP. Fig. 12 shows the bond stress versus free-end slip curves for these specimens. In this case CFRP sheets were first applied and then a certain degree of corrosion was imposed. The expansion caused by formation of corrosion products during the corrosion process is well confined by both stirrup and CFRP strengthening. A significant pressure is exerted on the surrounding concrete, and consequently the reactionary confinement and the mechanical interlocking of concrete around corroded steel bars is increased. Therefore, the maximum bond stress increases with the increasing degree of corrosion up to nearly 15% of degree of corrosion, which is quite clear from the regression results shown in Fig. 13. Simultaneously free-end slip at maximum bond stress is diminishing, as shown in Fig. 12, which indicates the interface area between rebar and concrete is getting denser and eventually the specimen failed in a more brittle way.

If a certain level of corrosion has been imposed before application of CFRP as in 25-R series, corrosion early products may leak out through expansion cracks in the post-repair corrosion process and thereby the expansion pressure is reduced. As a result, bond strength may not increase significantly from the formation of corrosion products, as shown in Figs. 12 and 13.

4. Conclusions

This study was performed to investigate the efficiency of CFRP strengthening to maintain and enhance the bond between corroded steel reinforcement and concrete both in short and long term. Based on the obtained results, the following conclusions can be drawn:

(1) Ultimate bond strength increases slightly in the early stage of reinforcement corrosion even without CFRP confinement. If corrosion continues ultimate bond strength decreases and the failure mode changes from bond splitting to rebar pullout.
(2) Corrosion induced bond deterioration without CFRP confinement strongly depends on test configuration; stirrup confinement can reduce the rate of bond deterioration.
(3) Corroded and strengthened specimens exhibit much higher ultimate bond strength as compared to similar but unstrengthened specimens, especially at medium and high levels of corrosion. Ultimate bond strength of series 25-S even increased with increasing degree of corrosion due to coupling effects of stirrup and CFRP strengthening.
(4) Most corroded specimens failed by rebar pullout after CFRP strengthening, with the exception of specimens subjected to severe corrosion.
(5) An increase of the ratio c/d_b up to a value of about 2.3 has a beneficial influence on the effect of CFRP strengthening. As the ratio c/d_b ratio increases beyond this threshold value, the confining effect of CFRP strengthening will decrease.
(6) As a result of CFRP confinement, ultimate bond strength increases with progressing corrosion up to a degree of corrosion of 15%. This effect was not observed on specimens with corrosion having taken place before strengthening. This could be explained by the occurrence of expansion cracking before strengthening, and the fact that corrosion products may leak out through these cracks. Both of these actions reduce the reactionary confinement.

Acknowledgment

The authors wish to express their gratitude and sincere appreciation to the Research Foundation for Young and Middle-aged Scientists of Shandong Province (No. BS2010SF027) for financing this research work.

References

[1] Du YG, Clark LA, Chan AHC. Impact of reinforcement corrosion on ductile behavior of reinforced concrete beams. ACI Struct J 2007;104(3):285–93.
[2] Azad AK, Ahmad S, Azher SA. Residual strength of corrosion-damaged reinforced concrete beams. ACI Mater J 2007;104(1):40–7.
[3] Mangat PS, Elgarf MS. Flexural strength of concrete beams with corroding reinforcement. ACI Struct J 1999;96(1):149–58.
[4] Almusallam AA, Al-Gahtani AS, Aziz AR. Effect of reinforcement corrosion on bond strength. Constr Build Mater 1996;10(2):123–9.
[5] Lee HS, Noguchi T, Tomosawa F. Evaluation of the bond properties between concrete and reinforcement as a function of the degree of reinforcement corrosion. Cem Concr Res 2002;32(8):1313–8.
[6] Cabrera JG, Ghoddoussi P. The effect of reinforcement corrosion on the strength of the steel/concrete bond. In: International conference, bond in concrete, from research to practice, vol.3. Riga, Latvia; 1992. p. 15–17.
[7] Hammoud R, Soudki K, Topper T. Bond analysis of corroded reinforced concrete beams under monotonic and fatigue loads. Cem Concr Compos 2010;32(3):194–203.
[8] Bonacci JF, Maalej M. Externally bonded fiber-reinforced polymer for rehabilitation of corrosion damaged concrete beams. ACI Struct J 2000;97(5):703–11.
[9] Kutarba MP, Brown JR, Hamilton HR. Repair of corrosion damaged concrete beams with carbon fiber-reinforced polymer composites. Composites 2004 Convention and Trade Show. Tampa, Florida, USA; 2004.
[10] Wang XG, Gu XL. Strengthening of corroding reinforced concrete beams by means of CFRP laminates. Restoration Build Monuments 2010;16(1): 47–56.
[11] Soudki K, Sherwood T. Bond behavior of corroded steel reinforcement in concrete strengthened with carbon fiber reinforced polymer sheets. J Mater Civil Eng 2003;15(4):358–70.
[12] Abdullah AA, Ahmad SA, Abdur RA. Effect of reinforcement corrosion on bond strength. Constr Build Mater 1996;10(2):123–9.
[13] Yuan YS, Yu S, Jia FP. Deterioration of bond behavior of corroded reinforced concrete. Ind Constr 1999;29(1):47–50.
[14] Fang CQ, Lundgren K, Chen LG, Zhu CY. Corrosion influence on bond in reinforced concrete. Cem Concr Res 2004;34(11):2159–67.
[15] Zhao YX, Jin WL. Test study on bond behavior of corroded steel bars and concrete. J Zhejiang Univ (Eng Sci) 2002;36(4):352–6.
[16] Chen LG, Fang CQ, Kou JX, Chen B. Bond property of reinforced concrete with corroded reinforcement. Ind Constr 2004;34(5):15–7.